Lasers in Surgery and Medicine 26:58–66 (2000)

Optical Integrating Balloon Device for Photodynamic Therapy

Peter J. Dwyer, MS,[1] W. Matthew White, BS,[1,2] Richard L. Fabian, MD,[1,2] and R. Rox Anderson, MD[1]*

[1]Wellman Laboratories of Photomedicine, Department of Dermatology, Massachusetts General Hospital, Harvard Medical School, Boston, Massachusetts
[2]Otolaryngology/Head and Neck Surgery, Massachusetts Eye and Ear Infirmary, Harvard Medical School, Boston, Massachusetts

Background and Objectives: **It is difficult to deliver light uniformly and efficiently over the complex shapes presented by various organs for photodynamic therapy (PDT). A balloon delivery device for photodynamic therapy was designed and tested for treatment of various anatomic tissues. The device uses the principle of optical integration by multiple internal diffuse reflections to achieve uniform output illumination.**
Study Design/Materials and Methods: **Soft, white, medical-grade silicone balloons were made in various shapes and tested for optical output, uniformity, efficiency, and power capabilities. Balloons were cast to be approximately the shape of the target tissue surface, organ, or cavity. Laser power was introduced into the saline-filled balloon by one or more fiber optics. Devices were constructed and used to illuminate oral mucosa and uterine endometrium for PDT.**
Results: **The balloon walls had low optical absorption, high diffuse reflectivity (80–95%), and low diffuse transmittance (5–20%) in the 500- to 900-nm wavelength region. Optical efficiencies of 65% were typical with emitted light over complex, nonspherical surfaces. Efficiency increased with inflation of the device, such that irradiance (power/area) at the balloon surface was nearly constant with inflation.**
Conclusion: **Optically integrating balloons can provide highly uniform, efficient light exposure over complex tissue surfaces. Uniformity and irradiance were not strongly affected by balloon inflation, and these robust devices are easy to produce in essentially any shape. Lasers Surg. Med. 26:58–66, 2000** **© 2000 Wiley-Liss, Inc.**

Key words: photodynamic therapy; laser; uniform illumination; balloon; cavity

INTRODUCTION

Photodynamic therapy (PDT) involves the therapeutic use of photosensitizing drugs activated by light at specific wavelengths [1]. From its clinical introduction in the early 1960s, PDT has grown into many different medical specialties [2–9]. A systemic, oral, or topical application of a light-sensitive drug or predrug is taken up into the target tissue. The drug is then activated by exposure to light delivered onto or into the tissue. Typically, the cytotoxic intermediate singlet oxygen is produced, which results in oxidative cell death. Tissue perfusion, which supplies oxygen, is generally required for effective PDT.

PDT was initially performed with broad-spectrum light sources such as xenon arc lamps or slide projectors [2,10] equipped with filters to transmit red wavelengths of light. Use of these

*Correspondence to: R. Rox Anderson, MD, Wellman Laboratories of Photomedicine, BHX 630, 50 Blossom Street, Boston, MA 02114.

Accepted 8 September 1999

TABLE 1. Existing Photodynamic Therapy Delivery Device Systems

Delivery device	Uniform irradiation (>70%)		Good efficiency (>60%)
	Simple surfaces*	Complex surfaces	
Cleaved tipped fibers			X
Microlens fibers	X		
Spherical tipped fibers			X
Cylindrical radiating fibers	X		X
Clear balloons with scattering medium	X		

*Simple surfaces are planar or cylindrical.

sources limits endoscopic uses, for example in the bladder, endometrium, or esophagus [5–8]. For endoscopic uses, lasers can be coupled efficiently to fiber optics, an exact wavelength can be generated to match the photosensitizer's absorption spectrum, and the higher power of laser light minimizes exposure time. Delivery of laser light to tissues can be accomplished by surface-illumination, intraluminal, or interstitially implanted fiber optic devices. Currently, there are commercially available optical fibers that have ends shaped and modified to create various beam profiles for treatment. Microlens, spherical tip, and cylindrical tip fibers are commonly used in PDT to irradiate the desired tissue.

Table 1 describes characteristics of typical PDT irradiation devices. Many of the existing optical delivery devices have (1) poor uniformity (less than or equal to 70%, calculated as described herein), (2) poor efficiency (less than or equal to 60%, calculated as power in/power out), and are (3) geometrically dependent. These values for the terms "good" and "poor" are not defined explicitly but are values that are considered reasonable and based on the authors' experience. Currently, most of the concerns with existing delivery devices have been with their inability to deliver light uniformly and efficiently over complex surface shapes. Required values of uniformity and efficiency are subjective depending on the laser, device, and tissue treated. It would be desirable to improve both of these values in PDT therapy to improve clinical response. Cleaved fibers and cylindrical diffusers have good efficiency (>85%) but moderate (70–80%) to poor (<70%) uniformity and are geometrically dependent. Clear balloons filled with a scattering medium are highly uniform (>95%) but have poor efficiency (<60%) and are still limited to simple surface shapes, such as a sphere. However, planar, spherical, and cylindrical shapes simply do not comply with many anatomic tissues. Light-delivery devices that force the tissue to assume a certain shape (cylinder or sphere) may compress and constrict the perfusion necessary for effective PDT. Because the drug by itself creates no cytotoxic effect, the efficacy of treatment depends largely on the accurate delivery of light directly to the target tissue. A uniform, efficient delivery device capable of conforming to complex tissue surfaces is lacking.

A delivery device, therefore, was designed, consisting of a soft silicone rubber balloon with titanium dioxide (TiO_2) particles (1- to 3-μm particle diameters) imbedded into the balloon material to provide optical scattering. The balloon can be a wide variety of shapes and is attached to a translucent nylon tube for insertion, inflation, and manipulation of the balloon into open areas. The TiO_2 particles create scattering sites in the wall material to give it high diffuse reflectance (R). Absorption of red light in the balloon wall is small, such that the wall's diffuse transmittance is $T \approx 1 - R$. The balloon is cast into a predetermined shape of the desired region to be treated. When deflated, the balloon device collapses for insertion into lumens, cavities, or other areas. Once positioned, the device can be gently inflated with saline and will conform to the tissue surface. The advantage of this system is that the balloon wall material does all the optical scattering in contrast to other balloons [11–13], where the medium does the scattering or the balloons are used just for positioning purposes. For odd shapes such as the uterus and the oral cavity, this device can efficiently deliver uniform laser irradiation, despite the extremely complex tissue surface shape.

Here, we report the construction and performance of these devices currently being used in clinical PDT trials involving the treatment of premalignant lesions in the oral cavity, and for treating dysfunctional uterine bleeding (i.e., destruction of the endometrial layer). These devices have potential applications for PDT in any hollow viscus, lumen, or complex surface such as oral, respiratory, genitourinary, gastrointestinal, pleural, and peritoneal cavities.

MATERIALS AND METHODS

Catheter System Design

Balloon catheter. The device design is based on the concept of optical integration, an ex-

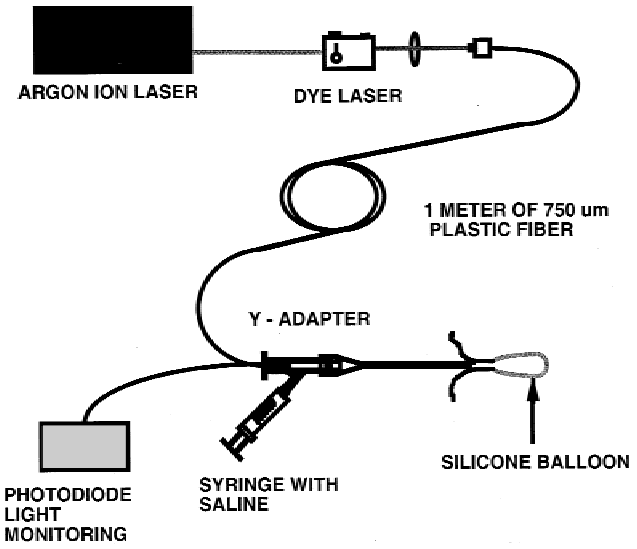

Fig. 1. Photodynamic therapy light delivery system.

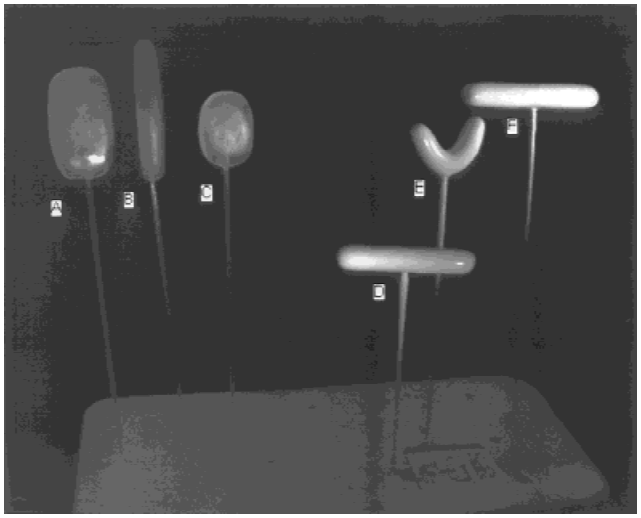

Fig. 2. Photodynamic therapy balloon device wax forms (**A,B,C**) and complete coated forms (**D,E,F**). Form A is used for the buccal mucosa and form E is used for the floor of the mouth.

ample is the integrating sphere, a sphere with a highly reflective coating on the inside to allow light to diffusely scatter around inside the sphere. This design produces nearly uniform illumination on the inner surface of the sphere. If a small percentage of this light were allowed to escape through the sphere wall, a uniform illumination would be achieved on the outside of the sphere. Furthermore, there is no absolute requirement that the shape be spherical. It is only necessary that the wall material has high diffuse reflectance, low transmission, and most importantly, low absorption. Inside the balloon, photons are scattered from the balloon wall many times. Low absorption, therefore, is essential to maximize the power output of the balloon and to minimize thermal effects. The higher the diffuse reflectance of the wall, the more the shape can deviate from spherical and yet maintain uniform light delivery over its surface. In practice, a delivery device whose shape can be altered severely for use in various anatomic regions and cavities in the body, requires the wall reflectance to be typically greater than 90%.

The balloon catheters we made consisted of two basic parts: (1) a flexible nylon tube used for manipulation, inflation of the balloon, and to carry the input optical fiber; and (2) a soft-shaped silicone balloon, which is attached to the tube (Fig. 1). The nylon tube (Putnam Plastics, Putnam, CT) had a nominal outer diameter of 2 mm and a nominal inner diameter of 1 mm. The proximal end of the tube was fitted with a female Luer Lock (Medical Disposables International, West Conshohocken, PA), which attaches to a "Y" port Tuey Borst adapter (Target Therapeutics, Fremont, CA) (see Fig. 1). This is where the saline dilation medium and the fiber optic delivery system are introduced into the catheter. A two-way stopcock was used at the syringe interface to the "Y" adapter to allow for catheter purging of air. The distal end of the nylon tube was sealed with a plug of acrylic epoxy to prevent the optical fiber, positioned inside the tube, from ever perforating the balloon. Along the distal walls of the tube, a series of staggered, 0.5-mm diameter holes were drilled, through which the saline enters or exits the balloon.

A simple way was devised to construct soft, white, medical-grade silicone rubber balloons to any shape desired, by using the lost wax technique (Fig. 2). Paraffin wax was warmed, then formed by hand to the shape desired. For example, uterine balloons were constructed based on ultrasound images of a patient's uterine cavity. A mixture of 12 ml of translucent medical grade silicone adhesive (NuSil, Carpinteria, CA), 1.5 grams titanium dioxide (TiO_2) powder with 1- to 3-μm-diameter particle sizes (Aldrich Chemical Company, Milwaukee, WIS) and 35 ml of ethyl ether anhydrous (Fisher Scientific, Pittsburgh, PA) was prepared in a 100-ml screw-top glass container. The components were stirred by hand, mixed thoroughly with an ultrasonic dismembrator (Artek Systems Corp., Farmingdale, NY), and then stirred with a magnetic Teflon mixing bar on

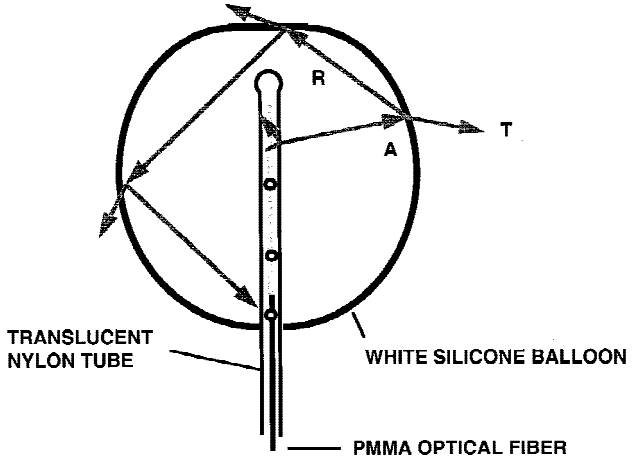

Fig. 3. Optical integration of balloon device. This diagram illustrates the possibility of photon absorption (A), reflection (R), or transmission (T) within the balloon cavity. PMMA, polymethyl methacrylate.

a stir plate for 8 hours to disperse the TiO_2 particles. In a nonsparking fume hood, a coat of the mixture was applied to the wax form by dipping the mold into the solution, allowing the excess to drip off and then placed in a rack to cure. Each coating was approximately 100 μm thick, and with multiple coating applications the balloon was made to any desired thickness. The common thickness used for oral and endometrial applications was approximately 300 microns. After curing overnight, the wax form was placed in boiling water to melt the wax, and the balloon membrane was flushed multiple times to remove wax residue. The balloons were dried and then positioned onto the prepared nylon tube, where the tube was rubbed with fine sandpaper at the point of attachment for better adhesion, and the same silicone/TiO_2 mixture was applied to the proximal section of the balloon to seal the balloon to the tube.

Optical fiber. The position of the optical fiber within the catheter/balloon system is shown in Figure 3. The optical fiber can have a cleaved-tip, cylindrical diffuser, or a ball tip preparation at the end of the fiber. The fiber used in our studies was a 0.5 numerical aperture, polymethyl methacrylate plastic fiber, with a core diameter of 500 μm and a cladding diameter of 550 μm (Asahi Chemical Industry Co., Tokyo, Japan). The proximal end of the fiber was terminated with a SMA 905 (Augat, Inc., Seattle, WA) fiber optic connector for alignment into a fiber chuck used for coupling laser light into the optical fiber. Under HeNe laser illumination, to view light exiting the optical fiber, the distal end of the plastic fiber was abraded gently with fine sandpaper to create diffuse, cylindrical irradiation for the intraballoon portion of the fiber.

Laser system. A Coherent Innova 100 argon-ion laser pumping a Coherent 599 dye laser (Coherent, Auburn, CA) tuned to the red region of the spectrum was used for optical tests of the device. All testing was performed at the PDT wavelengths of 630, 675, and 690 nm. The devices were also tested at 514 nm by using the argon laser. Laser light was coupled into the fiber system by using a 5× microscope objective with a 0.12 numerical aperture. The power from the optical fiber and the assembled balloon device was measured with a 5-inch diameter, calibrated integrating sphere radiometer by using a silicon photodiode detector (EG&G, Quebec, Canada).

Device Testing

Diffuse reflectance (R), transmission (T), and absorption (A) of all the components of the delivery device (balloon membrane, saline, and nylon tube) were assessed. A Beckman spectrophotometer (UV5270 Beckman Instruments, Fullerton, CA) with integrating sphere attachment was used to measure the balloon wall diffuse transmission and reflection (Fig. 3). Absorption was then determined by the relation

$$A = 1 - (R + T).$$

Scattering materials of titanium dioxide particles (TiO_2; 1- to 3-μm diameter), aluminum oxide ($Al_3 O_2$; 3-μm diameter), and zinc oxide (ZnO); 3.5-μm diameter), were compared by imbedding each scatterer into cast silicone rubber sheets made as described above, into 2.5 × 6 cm sheets of various thickness and measured for transmission and reflectance from 500 to 900 nm.

Optical efficiency of the devices was defined by the fraction of power delivered by the fiber, and the power emitted by the entire device. A test optical fiber was first placed into the sphere described above, at a known power output as measured by a calibrated power meter (Coherent, Auburn, CA). The catheter system and the entire balloon device were then placed into the sphere and the output measured. Uniformity of optical output from the balloons was measured with a linear, 8-bit charged coupled device camera (Pulnix model TM 745, Sunnyvale, CA) without AGC, with image processing software (NIH Image), and

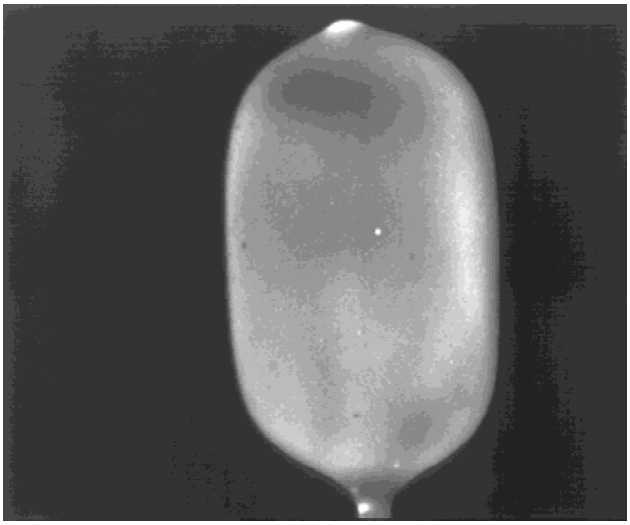

Fig. 4. Gray-scale image taken with a charged coupled device camera illustrates the uniformity of an oral balloon device.

a video capture board (Perceptics, Pixel Buffer, Knoxville, TN) installed in a PC. Images of an illuminated balloon device were captured, stored, and analyzed on the computer system (Fig. 4). The 8-bit resolution of the camera system allowed a maximal precision of 0.5% (0–255), and the camera aperture was adjusted to avoid saturation in the captured images. For example, Figure 4 illustrates a gray scale image of a balloon designed to treat the buccal mucosa area of the oral cavity. Uniformity was calculated as 1 minus the ratio of the standard deviation of pixel values divided by the mean pixel values

$$\text{Uniformity} = 1 - \text{SD/Mean}.$$

Different viewing angles were imaged with the charged coupled device camera system to ensure accurate uniformity measurements from planar surfaces within the depth of focus of the camera lens system.

Heating of each component in the optical radiation section of the balloon catheter and of the catheter system as a complete device was measured by using a calibrated infrared (thermal) camera (Inframetrics Corp., Bedford, MA), with 1.5 watts of optical input power. The devices were held in open air, which is a less conductive thermal medium than any biological tissue. Temperature rise under these conditions, therefore, is less than expected in any actual use. The device/components were monitored under constant illumination, from room temperature at the start of illumination, until equilibrium of temperature.

Deployment

The devices were cleaned with alcohol and gas sterilized before use on patients. For patient use, the optical fiber is prepared by placing the proximal, SMA connector end into a fiber X, Y, Z positioning alignment system for coupling of laser light into the optical fiber. The distal end of the optical fiber was placed in a calibrated integrating sphere as described above, where power adjustments can be made for appropriate treatment parameters. The Luer connector on the proximal end of the catheter tube was then attached to the exit port of the Tuey Borst "Y" adapter, and the illuminating fiber placed through the compression ring port of the "Y" adapter and advanced until properly positioned into the illuminating balloon. The compression ring on the adapter was then tightened to lock the fiber in place. To provide a low profile for insertion of the device into areas such as the uterus, the balloon was first deflated by using the syringe on the inflation port of the "Y" adapter. The catheter lumen was then sealed off to air by the two-way stop cock between the "Y" adapter and the syringe, placed into position under visual or ultrasound guidance, and the balloon gently inflated to conform to the tissue surface. Inflation pressure was always less than diastolic blood pressure to allow for blood flow in the target tissues. Once a treatment was complete, deflation of the balloon was performed by withdrawing the fluid through the syringe, and the device was withdrawn from the patient.

RESULTS

Figure 5 illustrates the reflection, and absorption of balloon walls containing the three scattering materials tested, over the 500- to 700-nm range. All three materials imbedded in silicone had flat, uniform spectral properties. The titanium dioxide/silicone mixture produced higher reflectance and lower absorption than the other two materials. The absorption of the balloon material was low in all cases; however, in the titanium dioxide balloons, absorption was less than a percent ($A < 1\%$). Figure 6 illustrates how the titanium dioxide material had increasing reflectance with increased balloon thickness. The ideal optical integration is produced as reflectance of the balloon wall approaches 100%. However, in practice, the optical efficiency decreases with more optical integration as photons interact more with the balloon wall material and the small, <1%

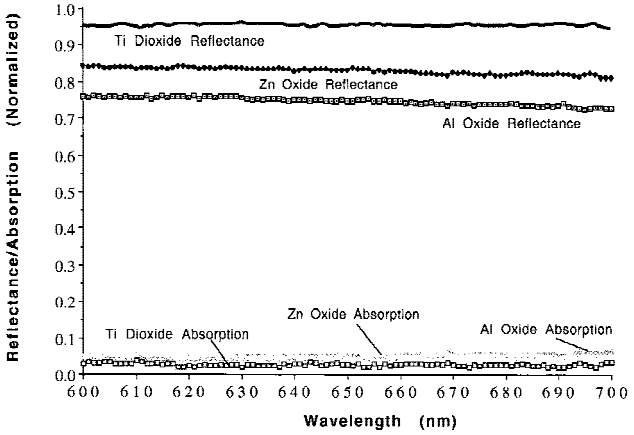

Fig. 5. Aluminum (Al) oxide, zinc (Zn) oxide, and titanium (Ti) dioxide imbedded into silicone material reflectance and absorption data. Titanium dioxide has a higher reflectance and lower absorption than the other materials; therefore, this is the scattering material used in all balloon devices.

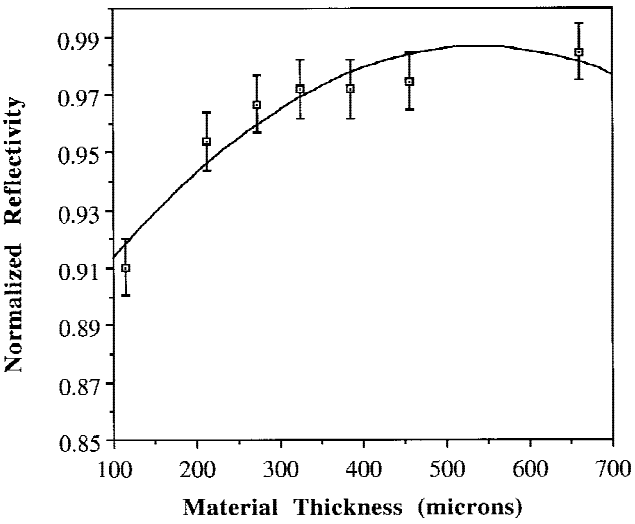

Fig. 6. Balloon material thickness strongly affected material reflectance. As the balloon material thickness increases, the material reflectance increases.

absorption becomes more significant. The approximate desired mechanical thickness of 300 μm provided a thin, conforming balloon that has low absorption and high enough reflectance (≈ 95%) to provide good uniformity even in odd shapes.

The linear gray scale images from the uniformity testing were analyzed by using the image processing software. The average uniformity for 17 different devices manufactured for the uterine and oral cavities were 93.4% with a standard deviation of 2.2%. Figure 7 illustrates the variation in uniformity over the devices tested. The balloons tested had an average thickness of 300 μm and variations, such as thick or thin areas within the same device, resulted in lowering uniformity values. Overall, the thinner the balloon material, the less uniform the device due to noticeable variations in coating thickness.

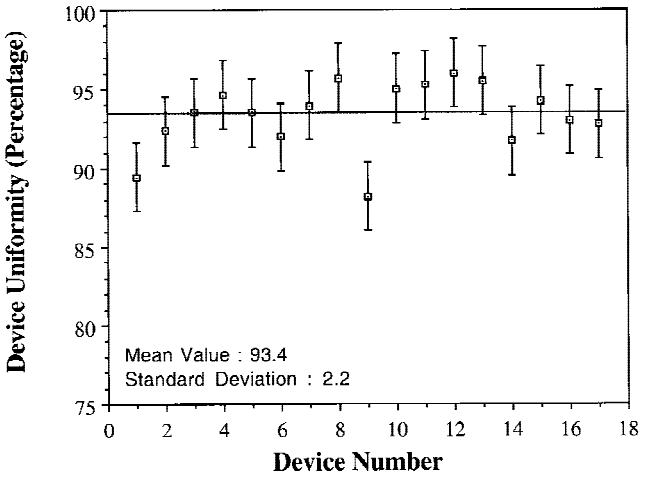

Fig. 7. Uniformity of 17 photodynamic therapy devices measured with a charged coupled device camera system. Average uniformity was 93.4% with standard deviation of 2.2%.

At 630 and 690 nm with a power of 1.5 watts entering the balloon, the center tube region achieved 47.2°C and the remaining sections of the catheter were near room temperature. The overall device (including the balloon) temperature, with the same laser parameters as previously discussed, slowly increase from 25°C to 47°C after 45 minutes. Optical efficiency of the titanium dioxide balloon was typically 65–75%. The maximal laser power capability of 3.5 watts of input (600–900 nm wavelength) was achieved without thermal damage to the devices. At this power, one device was monitored and increased temperature to 51°C after 45 minutes. These maximal temperatures are not high enough to induce thermal damage to the tissue. Typical output power of these devices is approximately 1.0–1.5 watts.

Balloon devices demonstrated increase in efficiency with increasing balloon inflation volume. As saline volume increases, the wall material stretches and thins, thus reducing the reflectivity, increasing the transmission and increasing efficiency of the device. The uniformity is slightly reduced when the device is inflated due to the thinning of the balloon wall. Small variations in the balloon wall become more apparent when the balloon is inflated beyond its normal distention. Typical increases in efficiency of uterine balloon devices were approximately 1.5% per ml of vol-

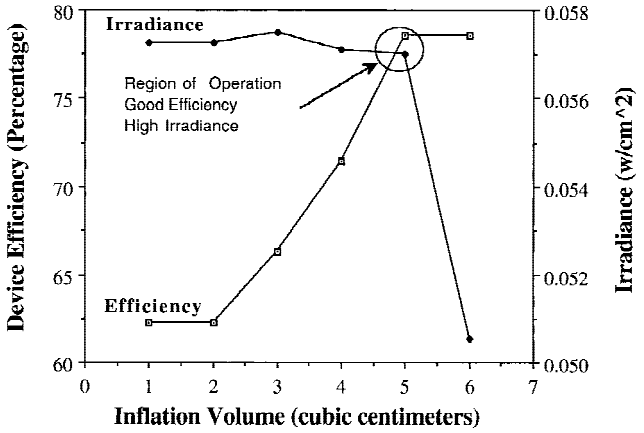

Fig. 8. Device efficiency and output irradiance over various inflation volumes. For this particular device, a 5-cc volume provided good efficiency with high irradiance.

ume extension of the balloon. Typical volume to fill the balloon without distension was 3 ml. Figure 8 illustrates the efficiency and irradiance versus inflation volume of a uterine device.

DISCUSSION

Many different types of delivery devices have been used in PDT, including multimode fibers with cleaved or polished ends [14], angled tips, and optical components attached to the end of the fiber to redirect the light [15]. These can be used intraluminally, or implanted interstitially into the target tissue. Cylindrical diffusers irradiate a field around the optical fiber axis [11,14] and were developed for tubular organs and structures such as esophagus. However, there is often considerable movement due to peristalsis, cardiac, and respiratory motion, which causes variable light dosimetry as the device and tissue shift their relative position. Centering balloon devices [11,12] were developed to keep the cylindrical diffusing fiber(s) near the center of the lumen, including a clear esophageal balloon for treatment of Barrett's esophagus. Other devices include a rigid, transparent Plexiglas bulb surrounding a cylindrical diffusing fiber, which forcefully stretches the esophagus to make the tissue uniformly smooth [13]. Allardice et al. used an esophageal dilator that was modified for light delivery in the esophagus [16]. There are also clear balloons with fluid-scattering media at various concentrations to optimize uniformity and efficiency [17]. Fiber ends can also be modified to shape the laser irradiation beam [18]. Scattering ball tip fibers have been used to produce a near isotropic source for treatment of round cavities such as the bladder. In these previous devices, the irradiance delivered to tissue is based on the geometry and exact positioning of the device and tissue [19–21]. Reflectance of the tissue also influences dosimetry. A direct method for monitoring dosimetry is to detect light with small fibers or detectors placed within the tissue [22,23], but this method samples only a very local region and is more invasive.

Our goal was to produce devices capable of nearly uniform, predictable light delivery over complex arbitrary, tissue shapes. Furthermore, we wanted soft, collapsible, and inflatable devices, in which the inflation pressure could be less than diastolic blood pressure, thus allowing tissue perfusion during PDT. The principle of optical integration by a highly diffuse-reflective balloon fulfilled these criteria well. Making the balloons by a simple casting process, we found that a wide variety of shapes were feasible. As the devices are inflated, both the balloon surface area and the optical efficiency increase such that delivered irradiance can be nearly independent of inflation volume.

Diffuse scattering in odd-shaped cavities is a complex process [24]. The goal of the balloon device is to optically integrate radiation from an optical fiber, uniformly over the shape of the balloon and tissue. In an optical integrating sphere, light incident on an area is diffusely reflected many times to uniformly illuminate the inside of the sphere. Although the theory is well understood for a sphere, it is not necessary for the device to be spherical, provided that the reflectivity is sufficiently high. The initial irradiance (E_i) on the inner surface can be calculated by using

$$E_i = P_i r/\phi A, \ (w/m^2/sr)$$

where r is the reflectance, P_i is the input power (watts), ϕ is the total projected solid angle (sr), and A is the area (m^2) of the illuminated surface. For an integrating sphere type device where multiple reflections occur, the incident irradiance on the surface of the balloon after the second reflection can be represented as

$$E_2 = P_i r^2/\phi A.$$

After n reflections, the total flux over the entire inner surface of the balloon can be written into a power series

$$E_n = (P_i r/\phi A)[1 + r + r^2 + \ldots + r^{n-1}] = (P_i r/\phi A)[1/1 - r].$$

Now the balloon surface radiance can be written as

$$L_s = TE_n = (TP_i r/\phi A)[1 + r + r^2 + \ldots + r^{n-1}] = T(P_i r/\phi A)[1/1 - r].$$

This equation can be used for any balloon device to calculate the radiance coming out of the balloon surface with input power P_i, an area surface A, inner surface reflectivity r, and transmission through the balloon wall T. To achieve uniformity over the inner surface of a sphere, it is necessary that the internal irradiance be significantly larger than the irradiance of the incident beam. In more complicated geometries, as in the case of the balloon devices, the above quantities are functions of position and the equations become more complicated. However in general, total irradiance is an infinite sum of contributions that depends on the internal reflectivity of the balloon material, the irradiance becomes more uniform as the number of reflections (n) increases, and the magnitude of the contributions falls off beyond n (proportional to 1/r).

The concept is highly effective and easily calculated when the shape is a sphere; however, as long as the wall reflectivity is high, the shape of the region can deviate from the sphere and still be highly effective in distributing light uniformly over the shaped cavity. Taking this approach one step further, if the sphere has a highly reflective wall, to reflect photons back into the interior and still has a small transmission through the wall, a uniform light distribution will be present on the outer surface of the sphere. In combining these two approaches, we achieved a balloon material made of silicone and titanium dioxide that has a high reflectivity (r = 98%) and a low transmission (T = 1%) wall that can be formed and inflated into a nonspherical shape. With the high radiance within the balloon due to the multiple reflections, the absorption within the balloon material and any other materials within the integration region has to be low to minimize thermal effects. This creates a conforming distribution of light that can effectively treat tissues. In the ideal case with no light absorption, the light interaction at the wall is either totally reflected back into the balloon cavity or delivered to the tissue. The light inside the balloon is reflected off internal components of the catheter without absorption and/or impinges on the balloon wall again. This process continues until the photon is transmitted out of the balloon membrane and into the tissue. All device temperature measurements were done in open air. In vivo, the device temperature may be higher due to initial tissue temperature. However, depending on the blood flow in the tissue, heat is carried away for tissue through conduction. The ambient temperature of the infused saline into the balloon, the blood flow in the tissue, and the time exposure of light determines the overall temperature of the balloon in vivo.

The balloon devices are an asset to PDT for essentially two reasons: (1) the ability to deliver uniform irradiance to the treatment area, and (2) enabling the calculation of a more accurate light dosimetry, because the true dose rate delivered directly to the tissue can be estimated in J/cm^2. Therefore, these robust devices can be used to treat odd-shaped cavities and provide safe, uniform, and efficient light exposures to PDT treatment regions. These devices, as opposed to conventional PDT devices, currently are being used in clinical trials for treating the endometrial layer of the uterus and the oral mucosa, due to the nonsymmetrical shape of the cavities. Preliminary observations show highly uniform destruction of desired tissue on these complex surfaces. More clinical studies in different specialties need to be performed to characterize these devices for efficacy and clinical significance.

REFERENCES

1. Henderson BW, Dougherty TJ. Photodynamic Therapy: basic principles and clinical applications. New York: Marcel Dekker; 1992.
2. Lui H, Anderson RR. Photodynamic therapy in dermatology: recent developments. Dermatol Clin 1993;11:1–13.
3. Gluckman JL. Photodynamic therapy for head and neck neoplasms. Otolaryngol Clin North Am 1991;24:1559–1567.
4. Wenig BL, Kurtzman DM, Grossweiner LI, et al. Photodynamic therapy in the treatment of squamous cell carcinoma of the head and neck. Arch Otolaryngol Head Neck Surg 1990;116:1267–1270.
5. Wyss P, Svaasand LO, Tadir Y, et al. Photomedicine of the endometrium: experimental concepts. Hum Reprod 1995;10:221–226.
6. Spitzer M, Krumholz BA. Photodynamic therapy in gynecology. Obstet Gynecol Clin North Am 1991;18:649–659.
7. Overholt BF. Laser and photodynamic therapy of esophageal cancer. Semin Surg Oncol 1992;8:191–203.
8. van Staveren HJ, Keijzer M, Keesmaat T, et al. Integrating sphere effect in whole-bladder wall photodynamic therapy: III. Fluence multiplication, optical penetration

and light distribution with an eccentric source for human bladder optical properties. Phys Med Biol 1996;41:579–590.
9. Dougherty TJ, Kufman JE, Goldfarb A, et al. Photoradiation therapy for the treatment of malignant tumors. Cancer Res 38:2628–2635.
10. Whitehurst C, Moore JV. Problems associated with the use of broad-band illumination sources for photodynamic therapy [letter]. Phys Med Biol 1996; 41:1518–1521; discussion 1521.
11. Panjehpour M, Overholt BF, Sneed RE, DeNovo RC, Petersen MG. A centering balloon to improve esophageal photodynamic therapy. Lasers Surg Med 1992;631–638.
12. Thomas RJ, Abbott M, Bhathal PS, St John DJB, Morstyn G. High-dose photoirradiation of esophageal cancer. Ann Surg 1987; 206:193–199.
13. Wagnieres G, Monnier P, Savary M, Cornaz P, Chatelain A, van den Bergh H. Photodynamic therapy of early cancer in the upper aerodigestive tract and bronchi: instrumentation and clinical results. SPIE Instr Ser 1990;IS6: 249–271.
14. McCaughan JS Jr, Nims TA, Guy JT, Hicks WJ, Williams TE, Laufman LR. Photodynamic therapy for esophageal tumors. Arch Surg 1989:124:74–80.
15. Lenz P. Light distributor for endoscopic photochemotherapy of tumors. Appl Opt 1987;26, 20:4452–4456.
16. Allardice JT, Rowland AC, Williams NS, Swain CP. A new light delivery system for the treatment of obstructing gastrointestinal cancers by photodynamic therapy. Gastrointest Endosc 1989;35:548–551.
17. Schmidt MH, Bajic DM, Reichert KW II, Martin TS, Meyer GA, Whelan HT. Light-emitting diodes as a light source for intraoperative photodynamic therapy. Neurosurgery 1996:38:552–556.
18. Murrer LH, Marijnissen JP, Star WM. Light distribution by linear diffusing sources for photodynamic therapy. Phys Med Biol 1996;41:951–961.
19. Beyer W. Systems for light application and dosimetry in photodynamic therapy. J Photochem Photobiol B 1996; 36:153–156.
20. Grossweiner LI. Light dosimetry model for photodynamic therapy treatment planning. Lasers Surg Med 1991;11: 165–173.
21. Grossweiner LI. Optical dosimetry in photodynamic therapy. Lasers Surg Med 1986;6:462–466.
22. D'Hallewin MA, Baert L, Marijnissen JP, Star WM. Whole bladder wall photodynamic therapy with in situ light dosimetry for carcinoma in situ of the bladder. J Urol 1992;148:1152–1155.
23. Werkhaven J, Harris DM, Krol G, Hill JH. Light dosimetry in animal models: application to photodynamic therapy in otolaryngology. Laryngoscope 1986;96:1058–1061.
24. van Staveren HJ, Beek JF, Keijzer M, Star WM. Integrating sphere effect in whole-bladder-wall photodynamic therapy: II. The influence of urine at 458, 488, 514, and 630 nm optical irradiation. Phys Med Biol 1995;40: 1307–1315.